

Orthogonal Waveform Space Projection Method for Adaptive Jammer Suppression

Kang-In Lee*, Hojun Yoon*, Jongmann Kim** and Young-Seek Chung†

Abstract – In this paper, we propose a new jammer suppression algorithm that uses orthogonal waveform space projection (OWSP) processing for a multiple input multiple output (MIMO) radar system exposed to a jamming signal. Generally, a conventional suppression algorithm based on adaptive beamforming (ABF) needs a covariance matrix composed of the jammer and noise only. By exploiting the orthogonality of the transmitting waveforms of MIMO, we can construct a transmitting waveform space (TWS). Then, using the OWSP processing, we can build a space orthogonal to the TWS that contains no SOI. By excluding the SOI from the received signal, even in the case that contains the SOI and jamming signal, the proposed algorithm makes it possible to evaluate the covariance matrix for ABF. We applied the proposed OWSP processing to suppressing the jamming signal in bistatic MIMO radar. We verified the performance of the proposed algorithm by comparing the SINR loss to that of the ideal covariance matrix composed of the jammer and noise only. We also derived the computational complexity of the proposed algorithm and compared the estimation of the DOD and DOA using the SOI with those using the generalized likelihood ratio test (GLRT) algorithm.

Keywords: MIMO radar, Bistatic MIMO radar, DOA estimation, Jammer suppression, ABF, GLRT

1. Introduction

There is growing interest in multi-input multi-output (MIMO) radar technologies for many military and wireless communication applications [1-8]. A MIMO radar system is composed of M_t transmitters and M_r receivers that can be collocated or spatially distributed [2-4]. Typically, a technique is used to enable each receiver to separate the reflected signals of interest (SOI) from each transmitter unambiguously through the use of orthogonal waveforms and a matched filter bank. Researchers have shown that orthogonal waveforms can be used in a MIMO radar system with spatially diverse transmitters and receivers to provide advantages in terms of target detection and parameter estimation compared with a traditional phased array system [9-11]. MIMO radar can achieve a higher resolution for collocated transmit and receive antennas than a phased array radar using the same number of physical antenna elements, because the MIMO radar has more degrees of freedom (DOF) than a phased array system with a single transmitting element [7-8].

With the development of a technique for monostatic radar cross section (RCS), however, the detection probability of monostatic radar has decreased. The use of bistatic MIMO radar has been studied extensively to solve this problem by separating the transmitter and receiver [12-16].

Conventional jammer suppression techniques for MIMO radar can be divided according to the use of two algorithms: the likelihood ratio test (LRT) based on a stochastic approach, and adaptive beamforming (ABF) that exploits a noise-jammer covariance matrix. While the ABF has a lower performance for SOI parameter estimation than the LRT, it has the comparative advantage in the computational complexity. However, the conventional ABF has a few limitations to suppress the jamming signals. First of all, when the received signal contains the SOI, conventional ABF suppresses the SOI simultaneously, which degrades the performance of the signal to interference plus noise ratio (SINR) [17]. Therefore, the covariance matrix for conventional ABF must be estimated from received signals without the SOI. In general, conventional ABF algorithms use the received signal for covariance matrix estimation immediately after or before transmitting the pulse. Also, since conventional ABF assumes that the jammer signal is homogeneous or uniform during applying the ABF, it can be vulnerable to fast fluctuating jamming signal.

To resolve these disadvantages above, we propose the orthogonal waveform space projection (OWSP) processing for MIMO radar, using the orthogonal transmitting waveforms. The proposed OWSP processing can build a noise-jammer covariance matrix for the ABF when the received signal in a pulse-repetition-interval (PRI) contains the SOI and the jamming signal simultaneously, by rejecting the SOI in the received signal. Therefore, the OWSP processing enables the ABF to suppress the jamming signals without additional SINR loss even if the SOI is included in received signal.

† Corresponding Author: Dept. of Electronic Convergence Engineering, Kwangwoon University, Korea. (yschung@kw.ac.kr)

* Dept. of Wireless Communications Engineering, Kwangwoon University, Korea. (kaang@kw.ac.kr)

** Agency for Defense Development, Korea. (jman95@add.re.kr)

Received: June 22, 2017; Accepted: October 16, 2017

To verify the proposed algorithm, we applied it to a bistatic MIMO radar system. And we applied the loaded sample matrix inversion (LSMI) beamformer as the ABF to the covariance matrix constructed using OWSP processing and estimated the DODs and DOAs of the SOIs for bistatic MIMO Radar system. We assumed that the noise and jamming signal have a random waveform, but some correlation with the waveform of the transmitter that passes through the matched filter. We also assumed that the jamming signal is stationary in each range bin for matched filtering and defined the correlation ratio of the SOI and jamming signal as the correlation coefficient, and studied the performance of the SINR and the estimation of the DOD/DOA after applying the ABF with respect to the correlation coefficient.

We also compared the SINR loss of the covariance matrix constructed using the proposed algorithm with that of the ideal covariance matrix composed of jammer and noise only. And we compared the DOD/DOA estimation performance after jammer suppression and the computational complexity with that of the GLRT.

2. Signal Model

For this investigation, we assumed that the signal bandwidth is small and that there is non-dispersive propagation. We also assumed that the waveforms that are transmitted are orthogonal to each other and that targets are represented by non-moving points.

Fig. 1 shows the configuration of bistatic MIMO radar. The signal received from the bistatic MIMO radar in a range bin composed of SOI, jammer and noise can be represented as [1,15]:

$$\mathbf{Y} = \sum_{s=1}^K \beta_s \mathbf{b}^*(\theta_s) \mathbf{a}^H(\phi_s) \mathbf{X} + \sum_{j=1}^{K_j} \alpha_j \mathbf{b}^*(\theta_j) \mathbf{J}_j + \mathbf{Z} \quad (1)$$

$$= \mathbf{Y}_S + \mathbf{Y}_J + \mathbf{Z}, \quad [M_r \times N]$$

$$\mathbf{X} = [\mathbf{x}_1; \mathbf{x}_2; \dots; \mathbf{x}_{M_t}]^T, \quad [M_t \times N] \quad (2)$$

$$\mathbf{x}_i = \{x_i(1), x_i(2), \dots, x_i(N)\}, \quad [1 \times N] \quad (3)$$

where

M_t, M_r : the numbers of transmitters and receivers, respectively

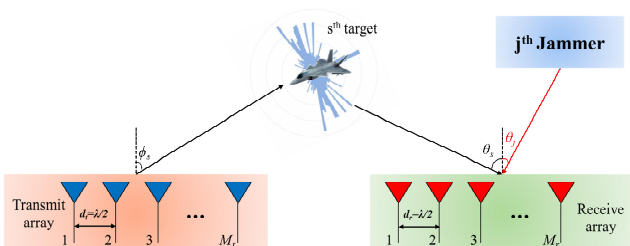


Fig. 1. Configuration of bistatic MIMO radar

- N : the number of transmitter waveform codes or data samples
- K : the number of SOIs
- K_j : the number of jamming signals
- ϕ_s : the direction of the s^{th} SOI from the reference transmitter (DOD)
- θ_s : the direction of the s^{th} SOI from the reference receiver (DOA)
- θ_j : the direction of the j^{th} jammer from the reference receiver.

In (1), \mathbf{Y} denotes the M_r -by- N signal matrix and \mathbf{X} the M_t -by- N transmitted waveform matrix, which is composed of the N -by-1 orthogonal waveform vector \mathbf{x}_i . Additionally, $\mathbf{a}(\phi)$ and $\mathbf{b}(\theta)$ are the steering vectors of the transmitting and receiving antenna array, with M_t -by-1 and M_r -by-1, respectively. β_s is the complex amplitude proportional to RCS of the s^{th} target. In (1), the first term \mathbf{Y}_S refers to the receiving matrix containing the target echo signals of the s^{th} target echo signal. And \mathbf{Y}_J denotes the receiving matrix for the jammer signals, \mathbf{J}_j the 1-by- N waveform vector and α_j the complex amplitude of the j^{th} jamming signal. The last term, \mathbf{Z} , is the spatially and temporally white circularly symmetric complex Gaussian noise sequence matrix with mean zero. $(\bullet)^*$ denotes the complex conjugate of a matrix.

3. Orthogonal Waveform Signal Projection Process

In this section, we propose the OWSP processing algorithm for constructing the noise-jammer covariance matrix when the received signal contains both the SOIs and jamming signal in MIMO radar. By exploiting the orthogonal transmitting waveforms of the MIMO radar, the target echo signals can be represented as a linear combination of the orthogonal transmitting waveforms. That is, the target echo signals are located in the TWS that is spanned by the orthogonal waveform vectors, which then become the basis vectors. By projecting the received signal onto the space orthogonal to the TWS, we can obtain the noise and jammer signals only, excluding the target echo signals. Then, we can construct the covariance matrix for adaptive beamforming.

The OWSP processing operator for the MIMO radar can be represented as [18]:

$$\mathbf{P}_\perp = \mathbf{I} - \mathbf{X}^T (\mathbf{X}\mathbf{X}^T)^{-1} \mathbf{X}, \quad [N \times N] \quad (4)$$

where \mathbf{P}_\perp is an orthogonal projection matrix subject to $\mathbf{X}\mathbf{P}_\perp = \mathbf{0}$. Multiplying (4) by (1) results in:

$$\hat{\mathbf{Y}} \equiv \mathbf{Y}\mathbf{P}_\perp = \sum_{s=1}^K \beta_s \mathbf{b}^*(\theta_s) \mathbf{a}^H(\phi_s) \mathbf{X}\mathbf{P}_\perp + \sum_{j=1}^{K_j} \alpha_j \mathbf{b}^*(\theta_j) \mathbf{J}_j \mathbf{P}_\perp + \mathbf{Z}\mathbf{P}_\perp, \quad [M_r \times N] \quad (5)$$

Because $\mathbf{X}\mathbf{P}_\perp = \mathbf{0}$ in (5), (5) can be simplified as:

$$\hat{\mathbf{Y}} = \sum_{j=1}^{K_j} \alpha_j \mathbf{b}^*(\theta_j) \mathbf{c}_j + \mathbf{C}_n, \quad [M_r \times N] \quad (6)$$

where $\mathbf{c}_j \equiv \mathbf{J}_j \mathbf{P}_\perp$ and $\mathbf{C}_n \equiv [\mathbf{c}_{n,1}; \mathbf{c}_{n,2} \cdots; \mathbf{c}_{n,M_r}] \equiv \mathbf{Z}\mathbf{P}_\perp$ are the correlation ratio of the jamming signal and the noise with respect to the transmitted waveform, respectively.

If the transmitted waveform matrix \mathbf{X} is not correlated with the jamming signal matrix $\mathbf{J} = [\mathbf{J}_1, \dots, \mathbf{J}_{K_j}]$, $[K_j \times N]$, then \mathbf{c}_j is equal to \mathbf{J}_j and there is no degradation in the jamming signal for the estimation of the covariance matrix. We can define the correlation ratio between the transmitted waveform matrix and jamming signal matrix as the correlation coefficient χ as follows:

$$\chi \equiv \frac{\|\mathbf{X}\mathbf{J}^H\|_2}{\|\mathbf{X}\|_2 \|\mathbf{J}\|_2} \quad (7)$$

In (7), $\|\cdot\|_2$ stands for the L_2 -norm of a matrix or vector. This correlation coefficient has a range of $0 \leq \chi \leq 1$. When $\chi = 0$, the transmitted waveform is orthogonal to the jamming signal, which means that there is no correlation between the transmitted waveform and jamming signal. Because the correlation coefficient may reduce the covariance matrix estimation performance, the ABF performance depends on the correlation coefficient χ .

Applying the LSMI to (6), the covariance matrix excluding the SOIs can be constructed as:

$$\hat{\mathbf{Q}} = \frac{1}{N} \hat{\mathbf{Y}}\hat{\mathbf{Y}}^H + \delta \mathbf{I}, \quad [M_r \times M_r] \quad (8)$$

where δ is the diagonal loading factor, which is about twice the noise power, and \mathbf{I} is the identity matrix [17]. In (8), $(\bullet)^H$ denotes the Hermitian transpose. Then, the optimal weight vector to reject the jamming signal can be evaluated as [19]:

$$\mathbf{w}(\theta_r) = \hat{\mathbf{Q}}^{-1} \mathbf{b}^*(\theta_r) \quad (9)$$

where θ denotes the scan angle within visible region. To verify the performance of the proposed covariance matrix (8), we introduced the SINR loss. From (8) and (9), the SINR can be derived as [17]:

$$\begin{aligned} SINR(\theta) &= \frac{\gamma_s |\mathbf{w}^H(\theta) \mathbf{b}(\theta)|^2}{\mathbf{w}^H(\theta) \left\{ \mathbf{E} \left[(\mathbf{Y}_J + \mathbf{Z})(\mathbf{Y}_J + \mathbf{Z})^H \right] \right\} \mathbf{w}(\theta)} \\ &= \frac{\gamma_s |\mathbf{w}^H(\theta) \mathbf{b}(\theta)|^2}{\mathbf{w}^H(\theta) \mathbf{Q} \mathbf{w}(\theta)} \end{aligned} \quad (10)$$

where

$$P_t = \frac{1}{N} (\mathbf{a}^H(\phi_s) \mathbf{X} \mathbf{X}^H \mathbf{a}(\phi_s)) \quad (11)$$

$$\gamma_s = \sum_{s=1}^K \beta_s P_t \quad (12)$$

In (10), the numerator $|\mathbf{w}^H(\theta) \mathbf{b}(\theta)|^2$ denotes the output power of the LSMI beamformer, and the denominator \mathbf{Q} is the ideal covariance matrix. $\mathbf{w}^H(\theta) \mathbf{Q} \mathbf{w}(\theta)$ is the output power of the beamformer by \mathbf{Q} . In (11), P_t represents the output power of the transmitter, which is proportional to the number of the transmitters in the MIMO radar [20]. In (12), γ_s is the signal power echoed from the target.

From (9) and (10), the SINR loss $L(\theta)$ is given as [17]:

$$\begin{aligned} L(\theta) &= \frac{SINR(\theta)}{SNR} = \frac{\sigma_n \gamma_s |\mathbf{w}^H(\theta) \mathbf{b}(\theta)|^2}{M_r \gamma_s \mathbf{w}^H(\theta) \mathbf{Q} \mathbf{w}(\theta)} \\ &= \frac{\sigma_n}{M_r} \frac{|\mathbf{b}^H(\theta) \hat{\mathbf{Q}}^{-1} \mathbf{b}(\theta)|^2}{\mathbf{b}^H(\theta) \hat{\mathbf{Q}}^{-1} \mathbf{Q} \hat{\mathbf{Q}}^{-1} \mathbf{b}(\theta)} \end{aligned} \quad (13)$$

where σ_n is the noise variance. We applied (13) to the proposed covariance matrix and ideal covariance matrix, and showed the degradation in the SINR loss of the proposed covariance matrix compared with that of the ideal covariance matrix.

4. Estimation of DOD and DOA Using LSMI Beamformer

In this section, we describe a method for estimating the DOD and DOA of the SOI from the beamformer output in the bistatic MIMO radar. In a conventional phased array, the beamformer output $\rho(\theta)$ refers to the output of the ABF at each scan angle and can be defined as the weight vector $\mathbf{w}(\theta)$ obtained from the ABF multiplied by the received signal matrix \mathbf{Y} in the array as [1]:

$$\rho(\theta) = \mathbf{w}^H(\theta) \mathbf{Y} \quad (14)$$

We can obtain DOAs by finding the peaks of (14) above a given threshold value on varying the scan angle within the visible region. To obtain the beamformer output for the bistatic MIMO radar, $\mathbf{w}(\theta)$ is multiplied by (1) and then:

$$\begin{aligned} \mathbf{w}^H(\theta) \mathbf{Y} &= \sum_{s=1}^K \beta_s \mathbf{w}^H(\theta) \mathbf{b}^*(\theta_s) \mathbf{a}^H(\phi_s) \mathbf{X} \\ &\quad + \sum_{j=1}^{K_j} \alpha_j \mathbf{w}^H(\theta) \mathbf{b}^*(\theta_j) \mathbf{J}_j + \mathbf{w}^H(\theta) \mathbf{Z} \\ &\approx \sum_{s=1}^K \beta_s \mathbf{w}^H(\theta) \mathbf{b}^*(\theta_s) \mathbf{a}^H(\phi_s) \mathbf{X} + \mathbf{w}^H(\theta) \mathbf{Z}, \quad [1 \times N] \end{aligned} \quad (15)$$

From (9), because $\mathbf{w}(\theta)$ becomes 0 near the jamming signal position θ_j , $\mathbf{w}^H(\theta_j) \mathbf{b}^*(\theta_s) \approx 0$ [17]. Here, $\hat{\mathbf{Q}}^{-1}$ is independent of the scan angle θ . Applying the matched filter to (15), we have:

$$\mathbf{w}^H(\theta) \mathbf{Y} \mathbf{X}^H \mathbf{a}(\phi) = \sum_{s=1}^K \beta_s \mathbf{w}^H(\theta) \mathbf{b}^*(\theta_s) \mathbf{a}^H(\phi_s) \mathbf{a}(\phi) + \mathbf{w}^H(\theta) \mathbf{Z} \mathbf{X}^H \mathbf{a}(\phi) \quad (16)$$

Eq. (16) can be represented as the multiplication of the beamformer output from the ABF and the beamformer output from the transmitting steering vector as follows:

$$\gamma(\theta, \phi) \equiv \mathbf{w}^H(\theta) \mathbf{Y} \mathbf{X}^H \mathbf{a}(\phi) \quad (17)$$

Applying the peak detection algorithm based on the difference in adjacent samples to (17), we can estimate the DOD and DOA within the visible region.

5. Computational Complexity

We derived the computational complexity of the proposed algorithm and compared it with that of the GLRT. The computational complexity can be approximated as the sum of the number of multiplications in the algorithm for:

$$C_p \approx M_r^3 + M_r^2 + N_\theta(M_r N) + N_\phi(M_t N + M_t) \quad (18)$$

where N_θ and N_ϕ is the number of angle samples in the visible region of DOA axis and DOD axis. The terms in (18) indicate the complexity due to (5), (8), (9), and (17), respectively. The complexity of the GLRT is given by [18]:

$$C_{GLRT} \approx \left[\begin{array}{l} M_r^3 + N_\theta(2M_r^2 + M_r) \\ + N_\phi(NM_r^2 + (2 + 2N)M_r M_t + M_t^2 + M_t) \end{array} \right] \quad (19)$$

In general, the complexities of the proposed algorithm and GLRT are proportional to the numbers of angle and data samples. If $M_r = M_t = M \gg 1$, $N \gg 1$, and $N_\theta = N_\phi \gg 1$, the difference between (18) and (19) can be approximated as:

$$C_{GLRT} - C_p \approx \left[\begin{array}{l} N_\theta M(2M - N) \\ + N_\phi M(3M + 3NM - N) \end{array} \right] \quad (20)$$

Also, when $N = \alpha M$ and $N_\theta = N_\phi = \beta M$, the ratio of (19) to (18) can be approximated as:

$$\frac{C_{GLRT}}{C_p} \approx \frac{3\alpha\beta M^4 + (5\beta + 1)M^3 + 2\beta M^2}{(2\alpha\beta + 1)M^3 + M^2 + 2\beta M} = O(M) \quad (21)$$

Eq. (21) shows that the complexity ratio is proportional to the number of antennas M . Fig. 2 shows the complexities of the two algorithms according to $M_t \times M_r$, with $N_\theta = N_\phi = 181$ in Fig. 2 (a) and $N_\theta = N_\phi = 361$ in Fig. 2 (b).

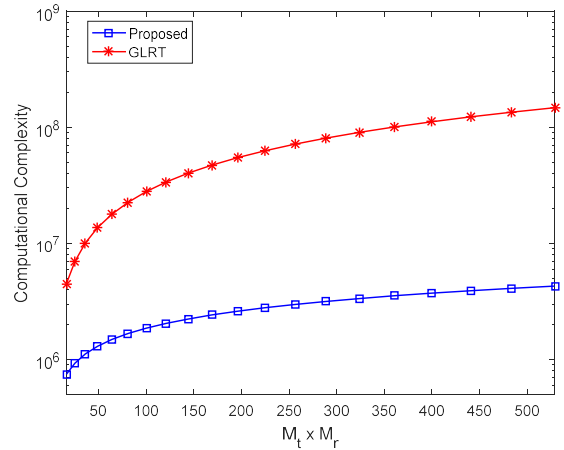


Fig. 2.(a) Comparison of complexities according to $(M_t \times M_r)$ with $N = 32$, $(N_\theta = N_\phi = 181)$

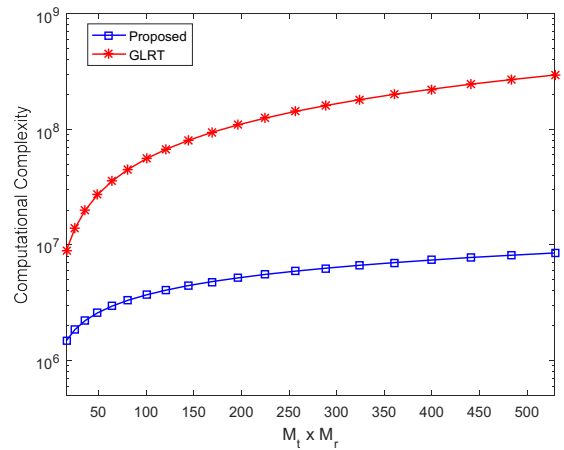


Fig. 2.(b) Comparison of complexities according to $(M_t \times M_r)$ with $N = 32$, $(N_\theta = N_\phi = 361)$

6. Numerical Examples

We used a linear array with uniform spacing for the receiving and transmitting arrays, with $M_t = 20$ and $M_r = 20$, respectively. We used $d_r = d_t = 0.5\lambda$ and $N_\theta = (361 \times 361)$. We also assumed that $\text{SNR} = 0 \sim 20$ dB, and the jammer-to-signal ratio (JSR) = 70 dB. We assumed that there are three target echo signals, with $\theta = (-10^\circ, 10^\circ, 30^\circ)$, $\phi = (20^\circ, 10^\circ, 0^\circ)$, and $\beta_s = (1.0, 1.0, 1.0)$, and that there are two jammer signals, with $\theta_j = (-20^\circ, 20^\circ)$. We assumed the noise is zero-mean white Gaussian noise. We also adopted an orthogonal binary phase shift keyed (BPSK) sequence based on the Walsh code, with $N = 32$ as the transmitted waveform. We used a random BPSK sequence with a Gaussian distribution as the waveform of the jammer signal.

Fig. 3 shows the SINR loss when JSR = 70 dB and SNR = 20 dB. The solid line shows the case of the SINR loss of the ideal covariance matrix, the dash-dot line the case of the proposed covariance matrix with $\chi = 0.95$, the dotted line

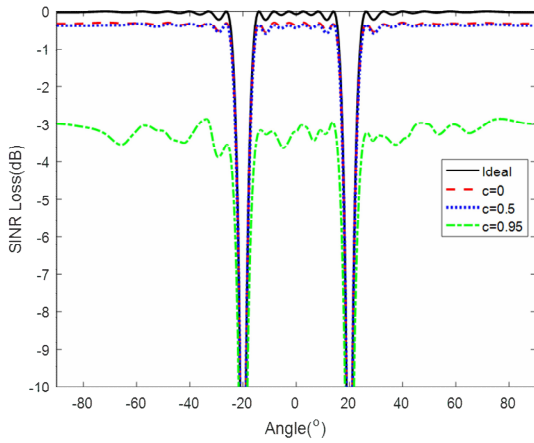


Fig. 3. SINR loss according to the correlation coefficient ($M_t=20$, $M_r=20$, and $N=32$ @ JSR=70dB and SNR = 20dB)

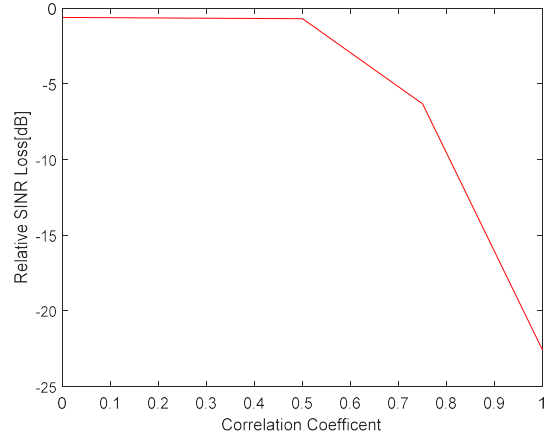


Fig. 4. Relative SINR loss according to the correlation coefficient ($M_t=20$, $M_r=20$, and $N=32$ @ JSR=70dB and SNR = 20dB)

the case of the proposed covariance matrix with $\chi=0.5$, and the dashed line the case of the proposed covariance matrix with $\chi=0.0$. The larger the correlation coefficient, the more the SINR loss is due to the increase in the correlation between the transmitted signal and the jamming signal.

To test the quality of the covariance matrix constructed using the proposed OWSP processing, we defined the relative SINR loss as follows:

$$\varepsilon_L(\chi) = 20 \log_{10} \sqrt{\frac{\int_{\Omega} |\mathbf{L}_{\text{est}}(\theta, \chi) / \mathbf{L}_{\text{ideal}}(\theta)|^2 d\theta}{N_{\theta}}} \quad (22)$$

where $\mathbf{L}_{\text{ideal}}(\theta)$ and $\mathbf{L}_{\text{est}}(\theta)$ are the SINR loss of the ideal and proposed covariance matrix, respectively, and Ω denotes the entire visible region. Fig. 3 shows the relative SINR loss according to the correlation coefficient. When $\chi \leq 0.5$, the SINR loss of the proposed covariance matrix is similar to that of the ideal covariance matrix, and the difference in the two SINR losses is less than -20dB.

Fig. 4 shows the mean square error (MSE) for the DOA and DOD estimation according to the SNR and the correlation factor. The MSE for the DOD and DOA estimation is defined as

$$\text{MSE} = \frac{1}{LK} \sum_{l=1}^L \sum_{k=1}^K \left\{ (\phi_k - \tilde{\phi}_{l,k})^2 + (\theta_k - \tilde{\theta}_{l,k})^2 \right\} \quad (23)$$

where $\tilde{\phi}_{l,k}$ and $\tilde{\theta}_{l,k}$ denote the estimated k^{th} DOD and DOA by the l^{th} trial, respectively. L is total number of Montecarlo trials and K is the number of SOIs. In Fig. 5, the MSE of GLRT is slightly smaller than that of the proposed algorithm, but the average computing time is 4.3 ms for the proposed algorithm, which is only 3% that of the GLRT at 137 ms. To compare the complexities of the two algorithms, we simulated 10,000 trials of the two algorithms on an Intel Core i7-6700 CPU @ 4.0 GHz.

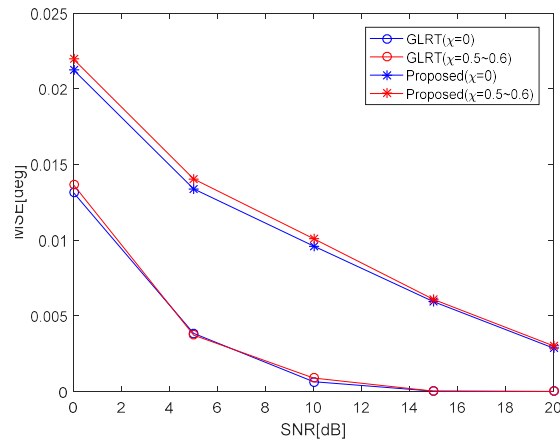


Fig. 5. MSE of the estimated DOD and DOA ($M_t=20$, $M_r=20$, and $N=32$, $N_{\theta} = N_{\phi} = 361$ @ JSR=70dB) after 10,000 trials

7. Conclusion

In this paper, we proposed a jammer-suppression algorithm that uses the Orthogonal Waveform Signal Projection (OWSP) processing algorithm based on the transmitted orthogonal waveform in MIMO radar. While conventional ABF algorithms require a covariance matrix that excludes the SOI, the proposed algorithm can remove the SOI from the received signal by using OWSP processing and construct a covariance matrix using the received signal without the SOIs. The proposed algorithm is verified by comparing the SINR loss using the proposed covariance matrix with that of an ideal one according to the correlation coefficient, which indicates the correlation ratio between the transmitted waveform and jamming signal. When the correlation coefficient is less than 0.5, the SINR loss of the proposed remains less than -5dB compared with that of the case with the ideal covariance matrix. With the

proposed algorithm, the MSE of the DOD and DOA estimations is similar to those of the GLRT, but the computational burden is less complex.

Acknowledgements

This work has been supported by the Low Observable Technology Research Center program of Defense Acquisition Program Administration and Agency for Defense Development.

References

- [1] J. Li and P. Stoica, "MIMO Radar Signal Processing," *Wiley*, 2008, pp. 1-64.
- [2] E. Fishler, A. Haimovich, R. Blum, D. Chizhik, L. Cimini, and R. Valenzuela, "MIMO radar: An idea whose time has come," in *Proc. IEEE Radar Conf.*, 2004, pp. 71-78.
- [3] A. M. Haimovich, R. S. Blum, and L. J. Cimini, "MIMO radar with widely separated antennas," *IEEE Signal Processing Magazine*, 2008, pp. 116-129.
- [4] J. Li and P. Stoica. "MIMO radar with collocated antennas," *IEEE Signal Processing Magazine*, 2007, pp. 106-114.
- [5] D. W. Bliss and K. W. Forsythe, "Multiple-input multiple-output (MIMO) radar and imaging: degrees of freedom and resolution," *Signals, Systems and Computers, 2004. Conference Record of the Thirty-Seventh Asilomar Conference on. IEEE*, 2003, pp. 54-59
- [6] ROBEY, Frank C., et al. "MIMO radar theory and experimental results," *Signals, Systems and Computers, 2004. Conference Record of the Thirty-Eighth Asilomar Conference on. IEEE*, 2004, pp. 300-304.
- [7] J. Li and P. Stoica, "MIMO radar — diversity means superiority (invited)," *Proc. 14th Annual Workshop on Adaptive Sensor Array Processing, MIT Lincoln Laboratory, Lexington, MA*, 2006.
- [8] L. Xu, J. Li, and P. Stoica, "Target detection and parameter estimation for MIMO radar systems," *IEEE Trans. Aerospace Electron. Syst.*, 2008, pp. 927-939.
- [9] J. Li, P. Stoica, L. Xu, and W. Roberts, "On parameter identifiability of MIMO radar," *IEEE Signal Process. Lett.*, 2007, pp. 968-971.
- [10] L. Xu, J. Li, and P. Stoica, "Target detection and parameter estimation for MIMO radar systems," *IEEE Trans. Aerospace Electron. Syst.*, 2008, pp. 927-939.
- [11] H. Wang, et al. "On parameter identifiability of MIMO radar with waveform diversity," *Signal Processing*, 2011, pp. 2057-2063.
- [12] N. J Willis. "Bistatic Radar," *SciTech Publishing*, 2005.
- [13] P. E. Howland. "Target tracking using television-based bistatic radar," *IEE Proceedings-Radar, Sonar and Navigation*, 1999, pp. 166-174
- [14] M. C. Jackson. "The geometry of bistatic radar systems," *IEE Proceedings F (Communications, Radar and Signal Processing)*, 1986, pp. 604-612.
- [15] M. Jin, G. Liao, and J. Li. "Joint DOD and DOA estimation for bistatic MIMO radar," *Signal Processing*, 2009, pp. 244-251.
- [16] H. Yan, J. Li, and G. Liao. "Multitarget identification and localization using bistatic MIMO radar systems," *EURASIP Journal on Advances in Signal Processing*, 2008.
- [17] W.-D. Wirth. "Radar Techniques Using Array Antennas," vol. 10: *IET*, 2001.
- [18] G. H. Golub, and F. Van Loan Charles. "Matrix computations," Vol. 3: *JHU Press*, 2012.
- [19] Y. Gu and A. Leshem. "Robust adaptive beamforming based on interference covariance matrix reconstruction and steering vector estimation," *IEEE Trans. Signal Processing*, 2012, pp. 3881-3885.
- [20] G. Fuhermann. "Transmit beamforming for MIMO radar systems using signal cross-correlation," *Aerospace and Electronic Systems. IEEE Transactions on*, 2008, pp. 171-186.



Kang-In Lee He received the B.S. degree in electronic engineering from Kwang-woon University, Seoul, Korea, in 2011. He is currently pursuing the Ph.D. degree via the combined M.S. and Ph.D. program in the School of Radio Science and Engineering, Kwang-woon University. His main research interests are the radar signal processing, phased radar system and microwave imaging techniques.



Hojun Yoon He received the B.S. and M.S. degree in electronic engineering from Kwang-woon University, Seoul, Korea, in 2015 and 2017. His main research interests are the radar signal processing, conformal array radar system.



Jongmann Kim He received the B.S. degree in electrical and electronics engineering from Kyungpook National University, Daegu, Korea, in 2002 and the M.S. degrees in electrical and electronics engineering from Pohang University of Science and Technology, Pohang, Korea, in 2004. From 2005

he has been in the Artillery for Defense Development, Daejeon, Korea. His main research interests are the radar system, detection and tracking.



Young-seek Chung He received his B.S., M.S., and Ph.D. degrees in electrical engineering from Seoul National University, Seoul, Korea, in 1989, 1991, and 2000, respectively. From 1991 to 1996, he was with the Living System Laboratory, LG Electronics. From 1998 to 2000, he was a Teaching Assistant of electrical engineering with Seoul National University. From 2001 to 2002, he was with Syracuse University, Syracuse, NY. From 2003 to 2005, he has been a faculty member with the Department of Communication Engineering, Myongji University, Kyunggi, Korea. He is currently a Professor of the Department of Electronics Convergence Engineering, Kwangwoon University, Seoul, Korea. His current interests are the radar signal processing and microwave imaging techniques.